Surv Geophys (2008) 29:37–50
DOI 10.1007/s10712-008-9041-3

ORIGINAL PAPER

GPS Height and Gravity Variations Due to Ocean Tidal Loading Around Taiwan

Ta-Kang Yeh · Cheinway ~~Huang~~ Hwang · Guochang Xu

Received: 29 November 2007 / Accepted: 20 August 2008 / Published online: 10 September 2008

Abstract This study presents predicts ocean tidal loading (OTL) effects using a Green's function approach and validates a novel tidal model for Taiwan. Numerical integration of OTL is performed using the Gauss quadrature method and a local tidal model for the inner zone and a global model for the outer zone. Observed time series of GPS-derived vertical displacements and gravity variations (3–7 days) at five co-located GPS-gravimeter stations along the South East China and Taiwan coasts were utilized to assess the accuracy of the proposed models and two other models. The OTL-induced gravity variations are 3–16 μgal and the vertical site displacements are 13–27 mm. Generally, an OTL model using a mixed global and local tidal model generates better agreement with the observations than an OTL model using a global tidal model only. However, containing a local model inside a global model does not always produce a good agreement with the observations. The relatively large discrepancies between modeled and observed OTL values at some stations indicate that there is a need for an improved local tidal model in the study area.

Keywords GPS · Gravimeter · Ocean tidal loading · Taiwan

1 Introduction

Ocean tides, under the influence of gravitation due to celestial bodies, are a phenomenon in which the ocean waves rise and fall regularly by following a certain cycle. The tides rise and

T.-K. Yeh (✉)
Institute of Geomatics and Disaster Prevention Technology, Ching Yun University,
No. 229, Jiansing Rd., Jhongli 320, Taiwan, ROC
e-mail: bigsteel@cyu.edu.tw

C. Huang
Department of Civil Engineering, National Chiao Tung University, No. 1001,
Tahsueh Rd., Hsinchu 300, Taiwan, ROC

G. Xu
Department of Geodesy and Remote Sensing, GeoForschungsZentrum Potsdam,
Telegrafenberg A17, 14473 Potsdam, Germany

fall twice a day, and the duration of each cycle varies depending on the place of observation. This phenomenon is related to the gravitational relationship between the Moon and the Earth. Ocean tides perform a braking action on the rotation of the Earth, slowing down the rotational speed. As the Earth is pulled by both the gravitational forces of the Sun and the Moon, part of the ocean water will rise. Such rising water will have to move faster so that it can catch up with the oceans when the Earth rotates. However, its speed cannot change and the Earth has to drag the water along when it rotates, which creates a resistance force called tidal friction. Tidal friction not only consumes tidal energy but also makes tides deform. Moreover, it gradually reduces the speed of the Earth's rotation.

The effects of ocean tidal loading (OTL) on gravity and site displacements are important for validating ocean tidal models and correcting temporal gravity changes in absolute and superconducting gravity measurements (Neumeyer et al. 2005), and for improving GPS positioning accuracy (Khan and Scherneck 2003). The OTL at any location near coastlines can be predicted using various global ocean tidal models and numerical algorithms. A summary of such resources can be found in Scherneck and Bos. Internet services for OTL computation are also available (e.g., http://www.oso.chalmers.se/∼loading/). These OTL predictions are largely based on global ocean tidal models. For a station along a coast, OTL modeling can be improved by including a local tidal model for the inner zone. Such a local tidal model must outperform its global counterpart in both accuracy and spatial resolution in order to be more useful for the local users. Other factors impacting OTL model performance are coastlines, numerical integration of the Green's function and interpolations of the nearest grid value (Bos and Baker 2005; Melachroinos et al. 2007).

This study is motivated by the recent introduction of two absolute gravimeters (Trademark: Micro-g FG5) and two superconducting gravimeters (Trademark: GWR) in Taiwan. For the best scientific outcome from absolute and superconducting gravity data, one must determine whether global ocean tidal models produce accurate OTL values and whether an improved loading model can be generated using local tidal models. For instance, Fig. 1 presents the tidal spectrum at the Hsinchu tidal station, which is dominated by the M_2 (semi-diurnal tide caused by the Moon) tide from the National Chiao Tung

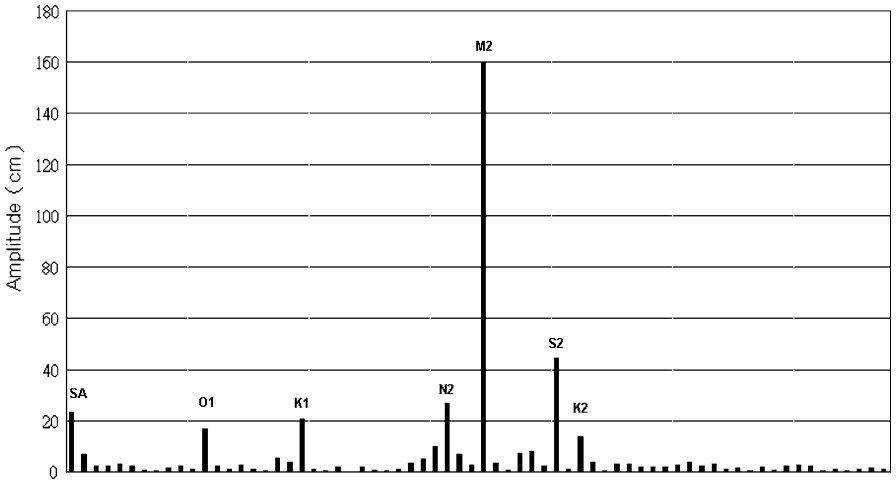

Fig. 1 Amplitude of the tidal spectrum at Hsinchu; the *x*-axis shows SA (solar semi-annual tides), O1 (lunar diurnal tides), K1 (lunar-solar diurnal tides), N2 (lunar elliptic tides), M2 (lunar semi-diurnal tides), S2 (solar semi-diurnal tides) and K2 (lunar-solar semi-diurnal tides)

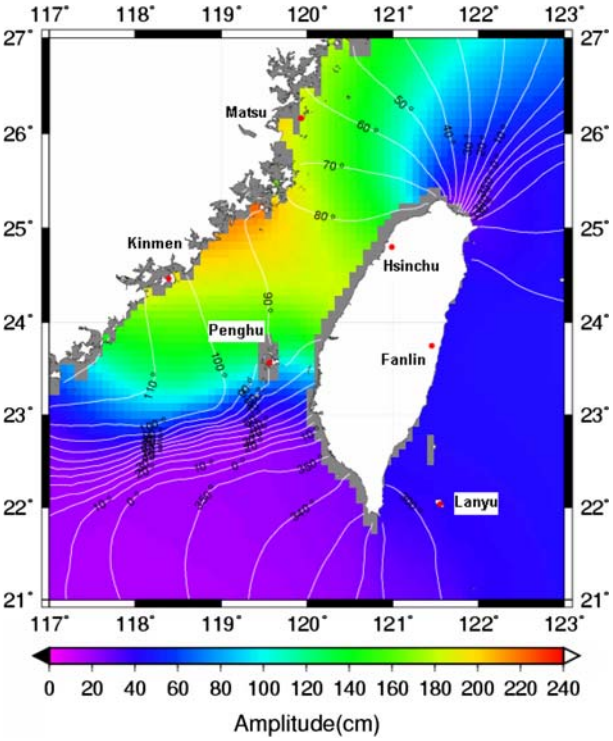

Fig. 2 M_2 tidal amplitudes and phases in the western Pacific, together with the positions of the five GPS and absolute gravimeter stations, shown in red

University NCTU1 combination. This combination uses the NAO.99b model (Matsumoto et al. 2000) for the outer zone effect and the NAO.99Jb model for the inner zone.

Figure 2 shows the amplitudes and phases of M_2 obtained by NCTU1 combination around South East China and Taiwan. The M_2 tide along the coasts of South East China and Taiwan is complex and contains high-frequency spatial variations in amplitude and phase (Fig. 2). Otherwise, when using a reference for the highest frequency variations, which can only be non-linear tides of the sub-diurnal tides. Adding to this complexity in the Taiwan Strait is the anomalous amplification of the M_2 tide and co-existence of progressive and standing M_2 waves (Jan et al. 2004). With this ocean tidal background, the goal of this study is to develop an improved OTL model for around Taiwan using the best possible tidal models, detailed coastlines and numerical techniques in order to provide the tidal parameters for the geophysical scientists. The accuracy of this proposed OTL model and selected global models is assessed using data collected by a Micro-g FG5 absolute gravimeter and GPS receivers at five stations along the coasts of South East China and Taiwan (Fig. 2).

2 Theory and Computation of Ocean Tidal Loading

This study employs the method using Green's functions (Farrell 1972) to compute the OTL effects on gravity and site vertical displacements. Compared with the spherical harmonic expansion method, this method is flexible in the joint use of local and global tidal models,

and in adapting a local, detailed coastline for loading computations. At any point $p(\theta_p, \lambda_p)$ on the Earth (θ_p, co-latitude; λ_p, longitude), gravitational change (L_g) and site displacements (L_r, radial; L_θ, northward; L_λ, eastward) due to OTL are (Farrell 1972):

$$L_g(\theta_p, \lambda_p) = \frac{g}{M} \iint_s \frac{\sigma(\theta, \lambda)}{4 \sin \frac{\psi}{2}} ds - \iint_s \sigma(\theta, \lambda) G(\psi) ds \tag{1}$$

$$L_r(\theta_p, \lambda_p) = \iint_s \sigma(\theta, \lambda) U(\psi) ds \tag{2}$$

$$L_\theta(\theta_p, \lambda_p) = \iint_s \sigma(\theta, \lambda) V(\psi) \cos A ds \tag{3}$$

$$L_\lambda(\theta_p, \lambda_p) = \iint_s \sigma(\theta, \lambda) V(\psi) \sin A ds \tag{4}$$

where $ds = \cos\theta d\theta d\lambda$ is the surface element, A is the azimuth, ψ is the spherical distance between point p and a running point at (θ, λ), and $\sigma(\theta, \lambda) = \rho_0 H(\theta, \lambda)$ is the surface density of the loading mass, with ρ_0, H being the average density of seawater (1.03 g cm^{-3}) and tidal height, respectively. The kernel functions (Green's functions) in Eqs. 1–4 are defined as (Farrell 1972):

$$G(\psi) = \frac{g}{M} \sum_{n=0}^{\infty} (2h_n' - (n+1)k_n') P_n(\cos\psi) \tag{5}$$

$$U(\psi) = \frac{R h_\infty'}{M} \sum_{n=0}^{\infty} P_n(\cos\psi) + \frac{R}{M} \sum_{n=0}^{\infty} (h_n' - h_\infty') P_n(\cos\psi) \tag{6}$$

$$V(\psi) = \frac{R l_\infty'}{M} \sum_{n=1}^{\infty} \frac{1}{n} \frac{dP_n(\cos\psi)}{d\psi} + \frac{R}{M} \sum_{n=1}^{\infty} (n l_n' - l_\infty') \frac{1}{n} \frac{dP_n(\cos\psi)}{d\psi} \tag{7}$$

where k_n', l_n', h_n' are the loading Love numbers of degree n, R and M are the average Earth radius and mass, g is the mean value of gravitational acceleration, and $P_n(\cos\psi)$ and $dP_n/d\psi$ are the Legendre function and its derivative, respectively. This study adopts the loading Love numbers as follows: the Han and Wahr (1995) model for degrees 2–696, and the Farrell (1972) model for degrees 687 to infinity.

The integrations of Eqs. 1–4 are implemented by the Gauss quadrature method (Press et al. 1993). This method is used for rigorous computation of the gravity terrain effect, and is a highly efficient and accurate numerical integration method. The Gaussian quadrature method yields results that outperform those obtained using the prism method (Xu 2007) and the Fast Fourier Transform (FFT) method (Corchete et al. 2007). The singular problem of the kernel function in the terrain correction is treated by considering the innermost zone effect, which can be expressed as a complete elliptic integral of the first kind. Given a computational domain (for the outer zone, the domain is always 0° to 360° longitude and −90° to 90° latitude), the Gauss quadrature method first computes the weight coefficients along the latitude and longitude directions. For a spherical surface integration, using $t = \cos\theta$ is convenient as the coordinate variable along the meridian. The weight coefficients are associated with coordinates where tidal heights are obtained by Newton-Gregory polynomial interpolation (Gerald and Wheatley 1994) from the given tidal grid. The kernel functions in Eqs. 5–7 are pre-computed as tables at a constant interval of 0.01° in latitude and longitude, and the needed function values are obtained by interpolation.

In the numerical integration, the total OTL effect is the sum of inner zone and outer zone effects. The inner zone effect uses a fine grid of tidal height (either from a local or global tide model) and the outer zone uses a coarse grid. Ideally, tidal heights for the inner zone should be from a local tidal model and those for the outer zone should be from a global tidal model. For convenience, an inner zone is defined as a rectangular box bordered by two meridians and two parallels of latitude. In this case, the latitude range is approximately 21°N to 25°N, and longitude range is roughly 120°E to 122°E. For the outer zone, the grid interval is always equal to that of the global tidal model. For example, the grid interval is 0.5° for the CSR4.0model (Eanes and Bettadpur 1996) and NAO.99b model (Matsumoto et al. 2000). Taiwan's coastline is defined by an 80 × 80 m digital elevation model (DEM). That is, the zero values of this DEM correspond to the Taiwan coastline. For southeast China, the coastline is defined by a high-resolution coastline of the Generic Mapping Tools (GMT) (Wessel and Smith 1999).

To obtain the most efficient and accurate model, various combinations of box size for the inner zone, and grid interval of the inner zone, are tested. When a global tidal model is utilized for the inner zone, the following choice has been found to be optimal in terms of efficiency and accuracy: box size = 3° and grid interval = 20′. When a local tidal model is used for the inner zone, the grid interval is equal to that implied by the model and the box size is 3°.

3 Choice of Global Tidal and Local Tidal Models

Numerous global tidal models are available for use in OTL computations. For instance, Andersen (1995) provided data of global ocean tides from ERS1 and TOPEX/Poseidon satellite altimetry, and the International Center for Earth Tides (ICET) provides OTL results for nine global models (http://www.astro.oma.be/ICET/Ocean_tides_models/index.htm). Due to the limited resources available for this study, the CSR4.0 (Eanes and Bettadpur 1996) and NAO.99b (Matsumoto et al. 2000) models are chosen for the experiments. Table 1 lists the current ocean tidal models. The CSR4.0 model is the standard model for tidal correction of TOPEX/Poseidon altimeter data. Notably, the NAO.99b model has been shown to outperform other tidal models in the western Pacific, partly due to the fact that this model assimilates tidal gauge data. Various local tidal models for the western Pacific exist (e.g., the NAO99.Jb model (Matsumoto et al. 2000) and JAN2004 (Jan et al. 2004)).

For OTL computations (Sect. 2), this study experiments with the CSR4.0 and NAO.99b models (for the global model), and NAO.99Jb and JAN2004 models (for the local model). Other models can be easily adapted to the OTL computations in this study. The tidal constituencies of both NAO.99Jb and JAN2004 are given on 5′ × 5′ grid. Although the NAO99.Jb model assimilates tidal gauge data, the JAN2004 model is purely based on the solutions of hydrodynamic equations and is part of the results generated by the Principle/al Ocean Model (POM) (Blumberg and Mellor 1987). Additionally, the JAN2004 model uses a 5′ × 5′ bathymetry model around Taiwan and other finely tuned parameters in the POM. According to Jan et al. (2004), the JAN2004 model (where the average RMS misfit is 0.123 m) has a better fit with tidal heights than the model proposed by Lefevre et al. (2000a) (where the average RMS misfit is 0.158 m) at 18 tidal gauges along the coasts of South East China and Taiwan.

Table 2 compares the amplitudes and phases of the M_2 tide from observations, and the CSR4.0, NAO.99b, NAO.99Jb and JAN2004 models at five tidal gauge stations, where FG5 and GPS data are used (Sect. 4). The NAO.99Jb model (67 mm error in amplitude at

Table 1 Lists of the current tidal models

Model	Area	Resolution	Type of solution
Schwiderski (Schwiderski 1980)	Global	1 by 1 degree grid	Hydrodynamic model, fit the tide gauges globally
NAO.99b[a] (Matsumoto et al. 2000)	Global	0.5 by 0.5 degree grid	Based on the same hydrodynamics model as the Schwiderski model, but has TOPEX/Poseidon data assimilated into it
FES94.1 (Le Provost et al. 1994)	Global	0.5 by 0.5 degree grid	Based on Schwiderski also, calculated on a finite element grid near the coast
FES95.2 (Le Provost et al. 1998)	Global	0.5 by 0.5 degree grid	Based on FES94.1, TOPEX/Poseidon data used to adjust the long wavelength
FES98 (Lefevre et al. 2000b)	Global	0.25 by 0.25 degree grid	Based on FES95.2, computed on a global grid instead of computing the ocean tides in a few ocean basins separately
CSR4.0[a] (Eanes and Bettadpur 1996)	Global	0.5 by 0.5 degree grid	Long wavelength adjustments of FES94.1 using TOPEX/Poseidon data, the spurious grid-cells over land having been removed
GOT00.2 (Ray 1999)	Global	0.5 by 0.5 degree grid	Long wavelength adjustments of FES94.1 using TOPEX/Poseidon data, and different in the polar regions because ERS1/2 data are used
TPXO.5 (Egbert et al. 1994)	Global	0.5 by 0.5 degree grid	Computed using inverse theory using tide gauge and TOPEX/Poseidon data
TPXO.6.2 (Egbert and Erofeeva 2002)	Global	0.25 by 0.25 degree grid	Based on TPXO.5, improved the resolution to 0.25 by 0.25 degree grid
NAO.99Jb[a] (Matsumoto et al. 2000)	Local	0.08 by 0.08 degree grid	Based on the same hydrodynamics model as the Schwiderski model, but has TOPEX/Poseidon data assimilated into it
JAN2004[a] (Jan et al. 2004)	Local	0.08 by 0.08 degree grid	Based on the solutions of hydrodynamic equations and is part of the results generated by the Principal Ocean Model

[a] The model employed in this study

Table 2 Comparison of amplitude (in mm) and phase (in degrees) of M_2 tide at five tide gauge stations along the coasts of South East China and Taiwan

Station	Item	Observation	NAO.99Jb	JAN2004	NAO.99b	CSR4.0
Hsinchu	Amplitude	1642	1575 (67)	1523 (119)	1820 (178)	1457 (185)
	Phase	86	86 (0)	83 (3)	85 (1)	97 (11)
Penghu	Amplitude	901	693 (208)	847 (54)	841 (60)	1023 (122)
	Phase	95	81 (14)	78 (17)	96 (1)	105 (10)
Lanyu	Amplitude	444	403 (41)	399 (45)	435 (9)	507 (63)
	Phase	302	297 (5)	297 (5)	310 (8)	316 (14)
Matsu	Amplitude	2071	2024 (47)	1951 (120)	2367 (296)	1803 (268)
	Phase	66	66 (0)	66 (0)	68 (2)	69 (3)
Kinmen	Amplitude	1749	1748 (1)	1877 (128)	1672 (77)	1248 (501)
	Phase	110	109 (1)	103 (7)	131 (21)	134 (24)

Values in parentheses show the difference between modeled and observed values

Hsinchu) agrees best with observations as it has a relatively higher resolution ($5' \times 5'$ grid for NAO.99Jb) than the other models and integrates tidal gauge data (Table 2). The performance of the JAN2004 model (119 mm error in amplitude at Hsinchu) is worse than that of the NAO.99Jb model, but is more accurate than the NAO.99b and CSR4.0 models. The NAO.99b model (178 mm error in amplitude at Hsinchu) also assimilates tidal gauge data, but it performs worse than the NAO.99Jb model due to its coarser spatial resolution (on a $30' \times 30'$ grid for the NAO.99b model). The CSR4.0 model (185 mm error in amplitude at Hsinchu), based on TOPEX/Poseidon altimeter data only, has the worst accuracy among the four models. The CSR4.0 model underestimates the amplitude of M_2 at Kinmen by 50 mm and the M_2 phase is in error by 24°.

Based on the result of amplitudes and phases of the M_2 tide (Table 2), this study adopts the NAO.99b model to determine the outer zone effect of OTL. Local models NAO.99Jb and JAN2004 are utilized to determine the inner zone effect. This study presents two novel combinations, NCTU1 and NCTU2. Both combinations use the NAO.99b model for the outer zone effect. For the inner zone, the NCTU1 and NCTU2 combinations use the NAO.99Jb and JAN2004 models, respectively. In other words, this study combines existing models to process the OTL problem around Taiwan. The OTL software developed by NCTU can use any tide model to determine inner and outer zone effects.

4 FG5 Gravity and GPS Measurements

The absolute gravity, GPS and tidal gauge data were collected during a campaign to establish an absolute gravity network around Taiwan. The campaign lasted from 1 November 2004 to 25 February 2005, and the observation time at the different stations varied from 3 to 7 days, depending on the available resources. The gravitational stations, which were co-located with continuous GPS stations, were only a few km from nearby tidal stations. Table 3 shows the approximate coordinates of the International Terrestrial Reference Frame (ITRF2000) of GPS, FG5 and tidal gauge stations. A Micro-g FG5 absolute gravimeter (serial number, 224) was employed to collect absolute gravity data. Gravitational measurements were made at 30-min intervals, with each dataset consisting of 50 drops. All environmental corrections, except OTL, were applied using Micro-g software

Table 3 The approximate ITRF2000 coordinates (in meters) of the GPS, FG5 and tide gauge stations

Station	Coordinate	GPS	FG5	Tide gauge
Hsinchu	X	−2982779.0	−2982769.7	−2973819.8
	Y	4966662.7	4966647.1	4972938.7
	Z	2658805.7	2658797.3	2656940.4
Penghu	X	−2886037.0	−3061828.5	−2885232.4
	Y	5087838.6	4984021.5	5088170.8
	Z	2534225.9	2534206.4	2534421.8
Lanyu	X	−3095830.7	−3095876.0	−3059694.3
	Y	5040454.4	5040408.1	5085482.5
	Z	2378375.5	2378326.9	2328141.0
Matsu	X	−2858574.6	−3030078.6	−2856672.4
	Y	4964558.4	4861766.7	4964785.9
	Z	2794722.4	2794706.4	2796115.8
Kinmen	X	−2761836.9	−2938497.4	−2753419.3
	Y	5110345.0	5010827.8	5117695.7
	Z	2625153.0	2625162.9	2619590.9

"g" v4.0 (Micro-g Solutions 2004). The observed air pressure was transferred to the normal air pressure using the barometric correction factor and the solid Earth tide was corrected by the ETGTAB model developed by Georg Wenzel (Faller 2002). When it came to the polar motion correction, the Earth orientation parameters could be obtained from the website of the International Earth Rotation and Reference Systems Service (IERS, http://maia.usno.navy.mil/).

Figure 3 shows the time series of the gravitational variation (without OTL corrections) at the five stations. The bold lines signify the gravitational data obtained by the FG5 gravimeter and the dotted lines show the predicted data derived by the NCTU1 combination. Moreover, the x-axis denotes time and MJD means the Modified Julian Date. Because the five stations are close to the sea and to the collision zone where the Eurasian Plate and the Philippine Sea Plate East of Taiwan meet, the scatter of the FG5 gravitational observations is roughly several μgal, compared to a sub-μgal scatter at a quiet site (for example, a site remote from the sea and free from nearby seismic activities). Despite the relatively large scatter, the M_2 loading signal at most stations is clearly visible in the time series.

The strategy for computing GPS coordinates is largely based on that developed by Khan and Scherneck (2003). The coordinates of the five GPS stations were determined using Bernese GPS software (Beutler et al. 2004). No OTL corrections were applied to a baseline solution relative to the Fanlin GPS station (Fig. 2). At this station, OTL displacements were removed using the NAO.99b ocean tidal model implemented using GOTIC2 software (Matsumoto et al. 2001). Furthermore, the International GNSS Service (IGS) sp3 precise ephemerides were used and the wet tropospheric correction applied for each hour for estimating the Zenith Troposphere Delay to GPS signals (Yeh et al. 2006). Fanlin is a continuous GPS station and its geocentric coordinates have been precisely determined in the ITRF2000 frame. The reference ellipsoid is the Geodetic Reference System of 1980 (GRS80) and the approximate coordinates of the Fanlin GPS station with respect to the origin at the Earth's center of mass are $X = -3048091.3$, $Y = 4983134.4$ and $Z = 2552645.0$ (in meters). This station was chosen as the reference station based on its small OTL. Therefore, the GPS-derived ocean loadings at the five stations are relative to the corrections from the NAO.99b model.

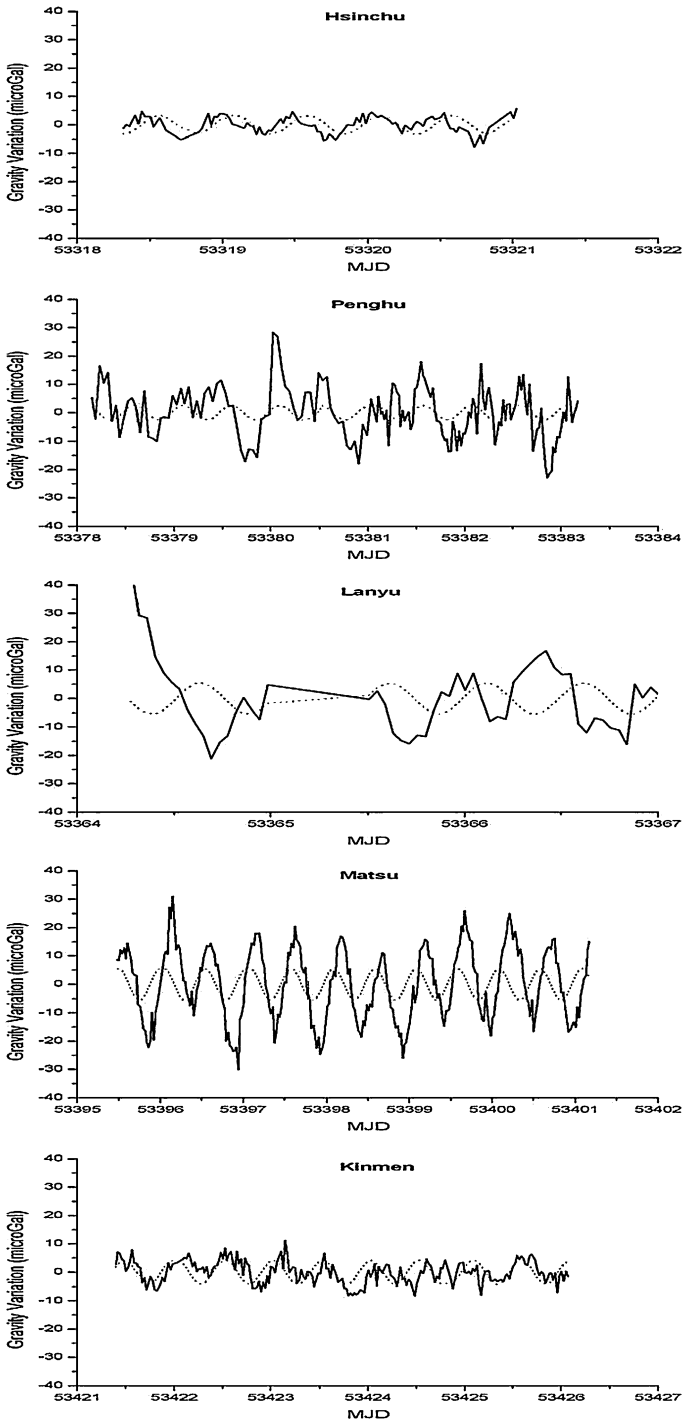

Fig. 3 Time series of FG5-observed (bold lines) and modeled (dotted lines) gravity variations, without ocean loading corrections

Figure 4 shows the time series of GPS height variations with a time-step of 3 h. The bold lines show height variations obtained via the GPS signals and the dotted lines present results predicted by the NCTU1 combination. The average formal standard errors of the 3-h GPS height solutions are 2.9, 3.3, 3.0, 2.7 and 3.9 mm for Hsinchu, Penghu, Kinmen, Matsu and Lanyu, respectively.

A number of sources contribute to variations in the time series for the GPS heights (Figs. 3 and 4), including, among others, tidal and non-tidal loadings, atmosphere loading, ground water table and data noise. Most of these sources generate variations with frequencies different from those of M_2. For instance, the atmospheric loading and wet troposphere-induced effect introduce diurnal variations in gravity and GPS coordinates, respectively (Neumeyer et al. 2005). Moreover, non-linear sub-diurnal tides exist in areas with shallow water, and an important energy transfer exists in the quart-diurnal (6 hourly) band (Melachroinos et al. 2007). Since this study focuses only on M_2 loading, signals or errors in the non-semidiurnal bands have little impact when investigating the M_2 loading based on the time series of gravity and GPS height values.

5 Comparison of Observed and Modeled M_2 Ocean Tidal Loadings

As the gravitational records are relatively short (3–7 days), only the M_2 OTL signals are extracted for model validation. A least-squares regression was applied to compute the amplitudes and phases of M_2 OTL from the time series of gravity values (Fig. 3) and GPS coordinates (Fig. 4) at the five stations. Table 4 compares the M_2 gravity OTL from the observations and from values generated by the NCTU, NAO.99b and GOTIC2 models. The GOTIC2 model uses the NAO.99b and NAO.99Jb models for the outer and inner zones, respectively (the same models are used by the NCTU1 combination, but with a different computational algorithm). Overall, the modeled amplitudes and phases generated by the NAO.99Jb model (NCTU1 combination) for the inner zone agree with the observations slightly better than the JAN2004 model (NCTU2 combination).

The modeled amplitudes and phases produced by the NCTU, NAO.99b and GOTIC2 models are generally consistent at all stations. At Hsinchu and Kinmen, which are located on opposite sides of the Taiwan Strait and at roughly the same latitude, the amplitudes generated by all models (3.0–3.5 μgal at Hsinchu and 3.5–4.3 μgal at Kinmen) agree well with the observations (3.1 μgal at Hsinchu and 3.7 μgal at Kinmen). However, a large difference in phase exists between all models (22.8–39.6 degrees at Hsinchu and 69.5–86.3 degrees at Kinmen) and the observations (66.4 degrees at Hsinchu and 125.0 degrees at Kinmen). At Penghu (central Taiwan Strait), the modeled amplitudes are approximately half the observed amplitudes, and the modeled phases agree well with the observed phases. At Lanyu (in the Pacific Ocean East of Taiwan), all modeled amplitudes are only $\sim$50% of the observed amplitudes, but the phases produced by NCTU1 and NCTU2 agree well with the observations. The largest discrepancy in amplitude between observation and model values occurs at Matsu (South East of the China coast), where the amplitudes generated by the NCTU1, NCTU2 and GOTIC2 models are only about 33% of the observed amplitude. However, the phases at Matsu produced by the NCTU combinations match the observations reasonably well.

These GPS solutions demonstrate that horizontal displacements from the GPS solutions are small (for the North direction the displacement is only 4.8–8.2 mm and for the East direction 8.8–19.5 mm). They are overwhelmed by noise in the data of around 2 cm

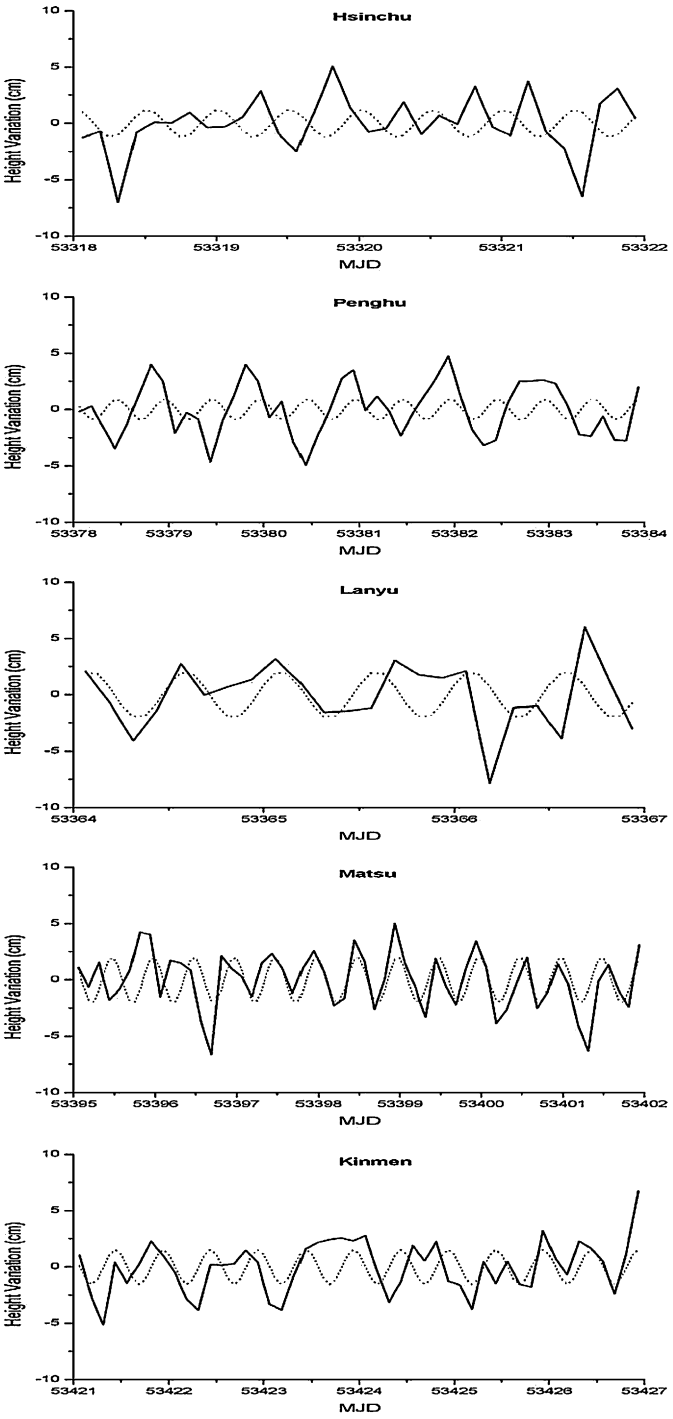

Fig. 4 Time series of GPS-derived (bold lines) and modeled (dotted lines) coordinate variations, without ocean loading corrections

Table 4 Comparison of amplitude (in μgal) and phase (in degrees) of modeled and observed gravity effects due to M_2 ocean tidal loading

Station	Item	Observation	NCTU1	NCTU2	GOTIC2	NAO.99b
Hsinchu	Amplitude	3.1 ± 0.2	3.3 (0.2)	3.1 (0.0)	3.0 (0.1)	3.5 (0.4)
	Phase	66.4 ± 3.9	30.9 (35.5)	22.8 (43.6)	39.6 (26.8)	33.8 (32.6)
Penghu	Amplitude	6.6 ± 0.4	2.6 (4.0)	2.6 (4.0)	3.0 (3.6)	3.4 (3.2)
	Phase	68.5 ± 3.5	70.4 (1.9)	59.7 (8.8)	64.7 (3.8)	60.4 (8.1)
Lanyu	Amplitude	11.9 ± 1.7	5.5 (6.4)	5.8 (6.1)	3.2 (8.7)	5.3 (6.6)
	Phase	348.3 ± 8.6	340.9 (7.4)	347.6 (0.7)	311.5 (36.8)	308.9 (39.4)
Matsu	Amplitude	15.7 ± 0.5	5.5 (10.2)	5.1 (10.6)	5.6 (10.1)	7.3 (8.4)
	Phase	67.2 ± 1.9	62.0 (5.2)	61.0 (6.2)	50.4 (16.8)	54.5 (12.7)
Kinmen	Amplitude	3.7 ± 0.2	4.2 (0.5)	3.7 (0.0)	3.5 (0.2)	4.3 (0.6)
	Phase	125.0 ± 2.9	86.3 (38.7)	69.5 (55.5)	85.6 (39.4)	84.5 (40.5)

Values in parentheses show the difference between modeled and observed values

(Yeh et al. 2007). Therefore, only the vertical displacement was examined. Table 5 compares modeled and observed vertical displacements due to M_2 OTL.

Compared with observed gravitational variations, the signal-to-noise ratios of the observed amplitudes and phases of the vertical displacements are relatively small; this is readily seen in the noisy time series of the GPS-derived coordinate variation (Fig. 4). Generally, all models produced similar results; the modeled amplitudes (11.3–13.1 mm at Hsinchu and 13.5–15.3 mm at Kinmen) agree well with the observed amplitudes (13.5 mm at Hsinchu and 18.0 mm at Kinmen). The differences between modeled phases (23.5–33.1 degrees at Hsinchu and 69.3–86.8 degrees at Kinmen) and observed phases (70.2 degrees at Hsinchu and 133.1 degrees at Kinmen) are relatively large compared with the gravitational loading (Table 4). At Lanyu, the phases generated by the NAO.99b and GOTIC2 models agree well with the observed phases; however, the NAO.99b and GOTIC2 models yield amplitudes that are only half of the observed amplitude.

Notably, the observations (Tables 4 and 5) show that the amplitudes of the OTL-induced gravitational variations and site displacements at Lanyu and Matsu are similar, and the values are roughly 10 μgal and 20 mm, respectively. Such a similarity applies to

Table 5 Comparison of amplitude (in mm) and phase (in degrees) of modeled and observed vertical displacements due to M_2 ocean tidal loading

Station	Item	Observation	NCTU1	NCTU2	GOTIC2	NAO.99b
Hsinchu	Amplitude	13.5 ± 4.8	12.1 (1.4)	11.3 (2.2)	13.1 (0.4)	12.8 (0.7)
	Phase	70.2 ± 20.9	32.1 (38.1)	23.5 (46.7)	32.4 (37.8)	33.1 (37.1)
Penghu	Amplitude	10.1 ± 2.4	9.2 (0.9)	8.9 (1.2)	12.1 (2.0)	12.1 (2.0)
	Phase	77.9 ± 9.9	73.5 (4.4)	61.9 (16.0)	57.9 (20.0)	59.8 (18.1)
Lanyu	Amplitude	27.4 ± 6.1	20.7 (6.7)	21.4 (6.0)	15.7 (11.7)	15.3 (12.1)
	Phase	313.7 ± 20.7	339.3 (25.6)	346.3 (32.6)	309.4 (4.3)	310.4 (3.3)
Matsu	Amplitude	25.2 ± 3.4	20.3 (4.9)	18.8 (6.4)	23.5 (1.7)	23.9 (1.3)
	Phase	76.9 ± 7.9	62.5 (14.4)	61.4 (15.5)	46.3 (30.6)	52.0 (24.9)
Kinmen	Amplitude	18.0 ± 5.2	15.3 (2.7)	13.5 (4.5)	13.5 (4.5)	13.9 (4.1)
	Phase	133.1 ± 18.7	86.8 (46.3)	69.3 (63.8)	81.1 (52.0)	82.0 (51.1)

Values in parentheses show the difference between modeled and observed values

Hsinchu, Penghu and Kinmen, where the amplitudes of the OTL-induced gravitational variations and site displacements are about 5 μgal and 10 mm, respectively.

Comparisons of the modeled and observed gravity effects and vertical site displacements due to M_2 ocean tidal loading (Tables 4 and 5) could not yield a conclusion regarding the ranking of model performance. Clearly, all OTL models under study require improvement. Although an OTL model using a mixed global and local tide model (NCTU1, NCTU2 and GOTIC2 models) outperforms a model with a global model only at some stations, it does not always produce the best results of OTL correction. An improved OTL model, in both precision and spatial resolution, can be created using improved local and global tide models, coastline data, loading Love numbers and better numerical techniques. As far as gravitational loading is concerned, the mismatch between observations and model-derived loading is partly attributed to the large scatter of the FG5 observations, which range from a few μgal to 10 μgal at the five stations. Finally, the large wet tropospheric effect on GPS solutions in tropical areas such as southeast China and Taiwan introduces significant uncertainty ($\sim$2 cm) in the GPS-derived vertical displacements. This then leads to an inconclusive comparison of modeled and observed vertical site displacements due to M_2 ocean loading (Table 5).

6 Conclusions

This study has presented the theory of and numerical technique for modeling ocean tidal loading (OTL) in Taiwan and nearby. Comparisons of observed and modeled OTL values at five almost co-located FG5-GPS stations indicate that the model-generated and observed values match well in some cases, but poorly in others. Generally, an OTL model using a mixed global and local tidal model produces better agreement with observations than an OTL model only using a global tidal model. The accuracy of the current OTL model for the coasts of South East China and Taiwan (Tables 4 and 5) demonstrates that the accuracy and spatial resolution of currently available tidal models need to be improved. The FG5 and GPS observations collected in this work are useful for validating improved OTL models in this region. Furthermore, observation intervals longer than 7 days should be used to have further improvements. The FG5 and GPS observations collected in this work are useful for validating improved OTL models in this region.

Acknowledgments The authors would like to thank the National Science Council of Taiwan, the Republic of China, for financial support of this research under Contract No. NSC95-2221-E-231-045. Moreover, Prof. Dr. Michael J. Rycroft (CAESAR Consultancy, Cambridge, UK) is appreciated for his valuable suggestions.

References

Andersen OB (1995) Global ocean tides from ERS 1 and TOPEX/POSEIDON altimetry. J Geophys Res 100(C12):249–259

Beutler G, Bock H, Brockmann E, Dach R, Fridez P, Gurtner W, Habrich H, Hugentobler U, Ineichen D, Meindl M, Mervart L, Rothacher M, Schaer S, Springer T, Urschl U, Weber R (2004) Bernese GPS software version 5.0 Draft, Astronomical Institute. University of Bern, Bern

Blumberg AF, Mellor GL (1987) A description of a three dimensional coastal ocean circulation model. In: Heap NS (eds) Three-dimensional Coastal Ocean Models, Coastal Estuarine Sciences, vol 4. American Goephysical Union, Washington, DC, pp 1–16

Bos MS, Baker TF (2005) An estimate of the errors in gravity ocean tide loading computations. J Geod 79:50–63

Corchete V, Chourak M, Hussein HM (2007) Shear wave velocity structure of the Sinai peninsula from Rayleigh wave analysis. Surv Geophys 28(4):299–324
Eanes RJ, Bettadpur S (1996) The CSR3.0 global ocean tide model: diurnal and semi-diurnal ocean tides from TOPEX/POSEIDON altimetry, CRS-TM-96-05. University of Texas, Centre for Space Research, Austin
Egbert GD, Erofeeva L (2002) Efficient inverse modeling of barotropic ocean tides. J Atmos Ocean Technol 19(2):183–204
Egbert GD, Bennett AF, Foreman MGG (1994) TOPEX/POSEIDON tides estimated using a global inverse model. J Geophys Res 99(C12):24821–24852
Faller JE (2002) Thirty years of progress in absolute gravimetry: a scientific capacity implemented by technological advances. Metrologia 39:425–428
Farrell WE (1972) Deformation of the earth by surface loads. Rev Geophys Space Phys 10:761–797
Gerald CF, Wheatley PO (1994) Applied numerical analysis, 7th edn. Academic Press, New York
Han D, Wahr J (1995) The viscoelastic relaxation of a realistically stratified earth, and a further analysis of postglacial rebound. Geophys J Int 120(2):287–311
Jan S, Chern CS, Wang J, Chao SY (2004) The anomalous amplification of M_2 tide in the Taiwan Strait. Geophys Res Lett 31:L07308. doi:10.1029/2003/GL019373
Khan SA, Scherneck HG (2003) The M_2 ocean tide loading wave in Alaska: vertical and horizontal displacement, modeled and observed. J Geod 77:117–127
Lefevre F, Provost C, Lyard FH (2000a) How can we improve a global ocean tide model at a regional scale? A test on the Yellow Sea and the East China Sea. Geophys Res Lett 105:8707–8725
Lefevre F, Lyard FH, Le Provost C (2000b) FES98: a new global tide finite element solution independent of altimetry. Geophys Res Lett 27(17):2717–2720
Le Provost C, Genco ML, Lyard F, Vincent P, Canceil P (1994) Spectroscopy of the world ocean tides from a finite-element hydrodynamic model. J Geophys Res 99(C12):24777–24797
Le Provost C, Lyard F, Molines JM, Genco ML, Rabilloud F (1998) A hydrodynamic ocean tide model improved by assimilating a satellite altimeter-derived data set. J Geophys Res 103(C3):5513–5529
Micro-g Solutions (2004) "g" Users manual, vol 4.0. Micro-g Solutions, Inc., Erie
Matsumoto K, Takanezawa T, Ooe M (2000) Ocean tide models developed by assimilating TOPEX/POSEIDON altimeter data into hydrodynamical model: a global model and a regional model around Japan. J Oceanogr 56:567–581
Matsumoto K, Sato T, Takanezawa T, Ooe M (2001) GOTIC2: a program for computation of oceanic tidal loading effect. J Geod Soc Jpn 47:243–248
Melachroinos SA, Biancale R, Llubes M, Perosanz F, Lyard F, Vergnolle M, Bouin MN, Masson F, Nicolas J, Morel L, Durand S (2007) Ocean tide loading (OTL) displacements from global and local grids: comparisons to GPS estimates over the shelf of Brittany, France. J Geod. doi:10.1007/s00190-007-0185-6
Neumeyer J, Pino J, Dierks O, Sun HP (2005) Improvement of ocean loading correction on gravity data with additional tide gauge measurements. J Geodyn 40:104–111
Press WE, Teukolsky SA, Flannery BP, Vetterling WT (1993) Numerical recipes, 2nd edn. Cambridge University Press, New York
Ray RD (1999) A global ocean tide model from TOPEX/POSEIDON altimetry: GOT99.2, NASA Technical Memorandum 209478
Schwiderski EW (1980) On charting global ocean tides. Rev Geophys Space Phys 18(1):243–268
Wessel P, Smith WHF (1999) The Generic Mapping Tools (GMT), technical reference and cookbook. University of Hawaii, Hawaii
Xu G (2007) GPS—theory, algorithms and applications, 2nd edn. ISBN 978-3-540-72714-9, Springer, Heidelberg
Yeh TK, Wang CS, Lee CW, Liou YA (2006) Construction and uncertainty evaluation of a calibration system for GPS receivers. Metrologia 43:451–460
Yeh TK, Wang CS, Chao BF, Chen CS, Lee CW (2007) Automatic data-quality monitoring for continuous GPS tracking stations in Taiwan. Metrologia 44:393–401

Journal : Small 10712 | Dispatch : 2-1-2009 | Pages : 1
Article No. : 9054 | LE | TYPESET
MS Code : GEOP71_ER | CP | DISK

Surv Geophys
DOI 10.1007/s10712-008-9054-y

ERRATUM

GPS Height and Gravity Variations Due to Ocean Tidal Loading Around Taiwan

Ta-Kang Yeh · Cheinway Hwang · Guochang Xu

1 Erratum to: Surv Geophys (2008) 29:37–50 DOI: 10.1007/s10712-008-9041-3

In the above-mentioned paper, which was published in Volume 29, No. 1 on pp. 37–50, a typing mistake of the second author's last name was not corrected. The name of the second author is Cheinway Hwang (not Cheinway Huang).

We sincerely regret this error and would like to make sure the correct information is published to increase the scientific value of the paper.

A1 The online version of the original article can be found under doi:10.1007/s10712-008-9041-3.

A2 T.-K. Yeh (✉)
A3 Institute of Geomatics and Disaster Prevention Technology, Ching Yun University,
A4 No. 229, Jiansing Rd., Jhongli 320, Taiwan, ROC
A5 e-mail: bigsteel@cyu.edu.tw

A6 C. Hwang
A7 Department of Civil Engineering, National Chiao Tung University, No. 1001,
A8 Tahsueh Rd., Hsinchu 300, Taiwan, ROC

A9 G. Xu
A10 Department of Geodesy and Remote Sensing, GeoForschungsZentrum Potsdam,
A11 Telegrafenberg A17, 14473 Potsdam, Germany